

## Coherent Two-Electron Spin Qubits in an Optically Active Pair of Coupled InGaAs Quantum Dots

K. M. Weiss, J. M. Elzerman,\* Y. L. Delley, J. Miguel-Sanchez, and A. Imamoglu

*Institute of Quantum Electronics, ETH Zurich, CH-8093 Zurich, Switzerland*

(Received 3 April 2012; published 6 September 2012)

In semiconductors, the  $T_2^*$  coherence time of a single confined spin is limited either by the fluctuating magnetic environment (via the hyperfine interaction), or by charge fluctuations (via the spin-orbit interaction). We demonstrate that both limitations can be overcome simultaneously by using two exchange-coupled electron spins that realize a single decoherence-avoiding qubit. Using coherent population trapping, we generate a coherent superposition of the singlet and triplet states of an optically active quantum dot molecule, and show that the corresponding  $T_2^*$  may exceed 200 ns.

DOI: 10.1103/PhysRevLett.109.107401

PACS numbers: 78.67.Hc, 42.50.Ex, 78.30.Fs

A single spin-1/2 particle such as an electron represents the prototypical two-level quantum system. However, its simplicity leaves no room for designing the energy levels to be robust against various sources of decoherence. This means single-spin coherence [1–6] can only be improved by dynamically decoupling the spin from its environment using echo techniques [6–9], or by reducing environmental fluctuations [10–12]. To bypass such elaborate procedures, we have to go beyond single-spin states and build robustness against decoherence directly into the energy spectrum [13]. In particular, coupling two electron [14,15] or hole [16] spins via a strong exchange interaction rewards us with a tunable energy spectrum that exhibits entangled spin singlet and triplet states [17,18]. The coupled system features a “sweet spot” in the bias parameters, where the qubit subspace spanned by the singlet state ( $S$ ) and the triplet state with spin  $z$  projection  $m_s = 0$  ( $T_0$ ) is first-order insensitive to magnetic as well as electric-field fluctuations, similar to what has been achieved in superconducting quantum circuits [19,20].

Although ground breaking experiments based on  $S - T_0$  states have been carried out using electrically defined coupled quantum dots (QDs), these were operated far from the sweet spot and with a minimal exchange coupling much smaller than the Overhauser field gradient [1,7,8,12]. Therefore, the  $S - T_0$  qubit was always exposed to either magnetic or electric-field fluctuations. In optically active QD molecules, on the other hand, experiments have been performed in the large-exchange regime, but still away from the sweet spot [14,16]. Here, we demonstrate for the first time that operation at the sweet spot is indeed a promising strategy, prolonging the  $T_2^*$  coherence time by two orders of magnitude. In fact, this system could be considered as a solid-state analog of atomic clock states [21]: The possibility of optical Raman coupling between the two clock states ( $S$  and  $T_0$ ) allows for manipulation of the qubit at the sweet spot where all unwanted low-frequency couplings vanish, ensuring full protection from noise.

Our experiments utilize a pair of tunnel-coupled self-assembled indium gallium arsenide QDs [17,22]. By adjusting the growth parameters [Fig. 1(a)], we ensure that both QDs are charged with a single electron for a wide range of the applied gate voltage  $V$ . In this so-called (1,1) regime [14–16], the  $S$  and  $T_0$  ground states [Fig. 1(b)] are split by a voltage-dependent exchange interaction  $E_{ST}$  [see the lower panel in Fig. 1(c)]. For a particular gate voltage  $V_0$  (the sweet spot),  $dE_{ST}/dV = 0$  so that  $E_{ST}$  is first-order insensitive to electric-field fluctuations. In addition, the large value of  $E_{ST}$  suppresses mixing between the  $S$  and  $T_0$  states arising from the Overhauser field gradient. Finally, hyperfine mixing between the three triplets ( $T$ ) is suppressed by applying an external magnetic field ( $B$ ) along the growth direction  $z$ , which splits off  $T_{\pm}$  (with spin  $z$  projection  $m_s = \pm 1$ ), while leaving both  $S$  and  $T_0$  unaffected. Under these conditions the two-level system of  $S$  and  $T_0$  is therefore extremely robust against both charge and nuclear-spin fluctuations and forms a decoherence-free subspace [13]. To demonstrate this experimentally, we focus on the lambda system formed by  $S$  and  $T_0$  plus the shared optically excited state  $R_+$  that contains a trion in the red QD [see the upper panel in Fig. 1(c)].

We employ single-laser differential reflection (dR) measurements [23,24] to map out the optical transitions of the red QD versus  $V$ . In the (1,1) regime we observe very efficient spin pumping into the  $S$  ( $T$ ) state while probing the  $T$  ( $S$ ) transitions, as evidenced by a vanishing dR contrast [Fig. 1(d)]. All transitions driven by a single laser are only visible in a narrow gate-voltage range at the edge of the (1,1) regime, where spin-flip tunneling processes to and from the back contact lead to spin relaxation between the ground states [15]. By having a resonant laser present on both the  $S - R_+$  and the  $T_0 - R_+$  transition simultaneously, the spin pumping is lifted and we can determine the voltage dependence of  $E_{ST}$  [inset to Fig. 1(d)]. From this, we find the sweet spot (indicated by the dotted red line) to be at  $V_0 = 190$  mV, just outside the (1,1) regime for this QD molecule (which we call CQD1).

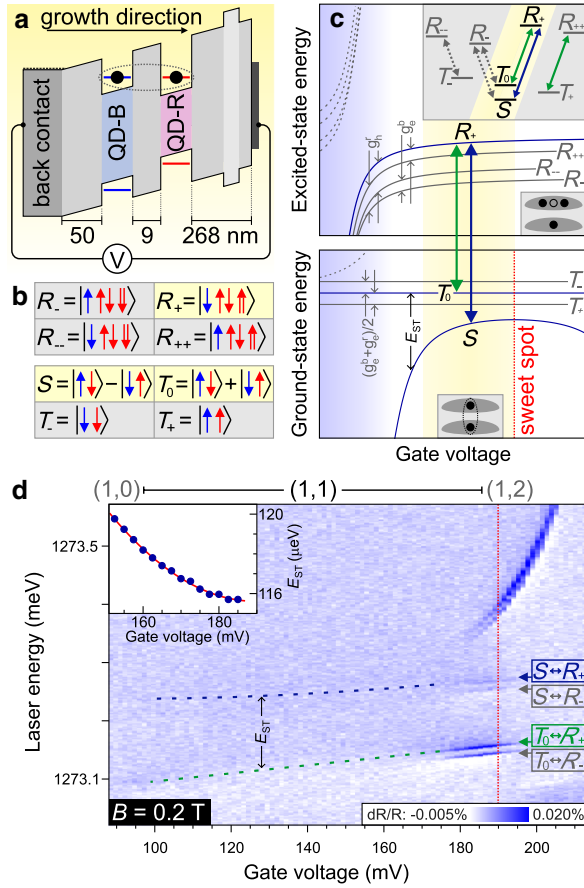


FIG. 1 (color online). (a) Schematic energy diagram of the device, containing two layers of self-assembled indium gallium arsenide QDs, separated by a 9 nm gallium arsenide tunnel barrier and embedded in a gallium arsenide Schottky diode. (b) Ground and lowest-lying optically excited states in the (1,1) regime. Blue arrows indicate electron spins in the bottom QD, red single (double) arrows indicate electron (hole) spins in the top QD. (c) Schematic energy diagram of the ground and optically excited states versus  $V$ . A magnetic field in Faraday geometry induces Zeeman splittings proportional to the  $g$  factors shown, with  $g_e^r$  ( $g_e^b$ ) denoting the electronic  $g$  factor in the red (blue) QD, and  $g_h^r$  the hole  $g$  factor in the red QD. The dotted red line indicates the sweet spot, where  $dE_{ST}/dV = 0$ . Inset: Circularly polarized dipole-allowed optical transitions between the states shown in (b). (d) Differential reflection (dR) measurement of the trion transitions in the red QD of CQD1 versus  $V$  at  $B = 0.2$  T, measured around saturation power (laser Rabi frequency  $\Omega = 0.8 \mu\text{eV}$ ) in the presence of a weak nonresonant (850 nm) laser. Blue (green) dashed lines indicate the  $S - R_+$  ( $T_0 - R_+$ ) transition energies, extracted from two-laser repump measurements [23], and the dotted red line indicates the sweet spot. The unmarked diagonal feature in the top right-hand corner is due to indirect transitions involving the (1,2) charging ground state. Inset:  $E_{ST}$  versus  $V$ , including a parabolic fit (red line).

In order to measure the coherence properties of the two-level system formed by  $S$  and  $T_0$ , we rely on the quantum optical technique of coherent population trapping (CPT) [25,26]. A weak probe laser is tuned across the  $S - R_+$

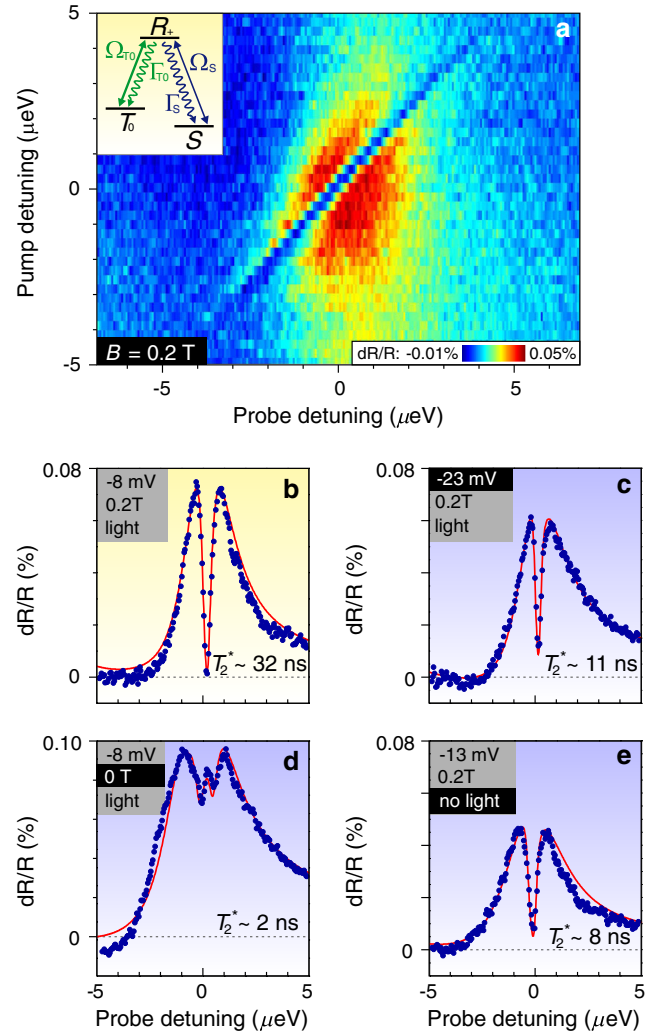


FIG. 2 (color online). Coherent population trapping with an  $ST$  qubit (CQD1). (a) CPT measured in dR versus pump and probe laser detuning at  $\Delta V = -13$  mV and  $B = 0.2$  T. The probe laser ( $\Omega_S = 0.34 \mu\text{eV}$ ; incident on the  $S - R_+$  transition) and the pump laser ( $\Omega_{T_0} = 0.83 \mu\text{eV}$ ; incident on the  $T_0 - R_+$  transition) have orthogonal linear polarization. Inset: Schematic diagram of the right-hand circularly polarized lambda scheme. (b) dR (blue dots) versus probe detuning at  $B = 0.2$  T and  $\Omega_{T_0} = 0.77 \mu\text{eV}$ , in the presence of a weak nonresonant (850 nm) laser that reduces the charge fluctuations. A numerical fit (red line) to an eight-level model [23] gives the  $T_2^*$  time indicated. (c) Same as in (b), but with  $\Omega_{T_0} = 0.58 \mu\text{eV}$  and  $\Delta V = -23$  mV. (d) Same as in (b), but at  $B = 0$  T. (e) Same as in (b), but at  $\Delta V = -13$  mV and without the nonresonant laser.

transition while a nonperturbative coupling laser is incident on the  $T_0 - R_+$  transition [see the inset to Fig. 2(a)]. At the two-photon resonance the QD molecule is prepared in an optically dark state consisting of an antisymmetric superposition of  $S$  and  $T_0$ . Here destructive interference between the two optical transition paths leads to a vanishing photon scattering amplitude, and thus a dip (or dark resonance) in the dR spectrum [Fig. 2(a)]. Because this

transparency results from the formation of a coherent superposition of  $S$  and  $T_0$ , decoherence processes with both slow and fast decorrelation times lead to a suppression of the CPT dip.

We observe that the  $S - T_0$  coherence is highly sensitive to the external magnetic field and the applied gate voltage. At  $B = 0.2$  T and  $\Delta V = V - V_0 = -8$  mV, the CPT dip goes completely to zero for a pump laser Rabi frequency of  $\Omega_{T_0} = 0.77$   $\mu\text{eV}$  [Fig. 2(b)]. Tuning  $V$  away from the sweet spot to  $\Delta V = -23$  mV yields dephasing due to electric-field fluctuations, leading to a reduced depth of the CPT dip and a general broadening of the dR spectrum [Fig. 2(c)]. We find that the electric-field fluctuations, which are probably due to rapid filling and emptying of charge traps around the QD, are reduced by illuminating the sample with a weak nonresonant (850 nm) laser [27]; switching this laser off thus results in a reduced CPT dip even quite close to  $V_0$  [Fig. 2(e)]. Most strikingly, by tuning the magnetic field to a value below that of typical nuclear Overhauser fields ( $B_n \sim 20$  mT), we find that the single strong dark resonance turns into two shallow transparency dips [Fig. 2(d)]. In this regime, the in-plane component of  $B_n$  ensures that  $T_+$  and  $T_-$  gain some  $T_0$  character, enabling the formation of two extra quasidark states, which are no longer immune to slow Overhauser field fluctuations; in Fig. 2(d), the leftmost of the resulting three dips is obscured due to the small but finite detuning of the pump laser. Applying a large enough external in-plane magnetic field would fully suppress the  $T_0$  character of the middle one of the three modified  $T$  states [18], yielding two dark resonances with a controllable splitting.

To quantify the coherence time, we measure the CPT dip for different pump laser powers and gate-voltage detunings (Fig. 3). The results are then analyzed by numerically solving the optical Bloch equations [23] for the full eight-level system shown in Fig. 1(b). We find that there are two qualitatively different decoherence mechanisms with a very similar effect on the line shape of the CPT dip. Far away from the sweet spot [Fig. 3(a)], the coherence is limited by Gaussian charge fluctuations (with standard deviation  $\delta V = 0.6$  mV and long decorrelation time) that lead to fluctuations in  $E_{ST}$ , resulting in a spin dephasing time  $T_2^* = 11$  ns [Fig. 3(c)]. Moving closer towards the sweet spot [Fig. 3(b)], the effect of the charge fluctuations becomes weaker. However, spin-flip tunneling with the back contact [15] now becomes stronger, because in this coupled QD pair the sweet spot is located very close to the edge of the (1,1) regime. We capture this in our model by including an additional Markovian spin dephasing term  $T_2^{\text{tunnel}} = 250$  ns, leading to  $T_2^* = 32$  ns [see Fig. 3(d)]. We note that a single CPT trace is not sufficient to distinguish between the two decoherence mechanisms and thus cannot give a reliable value for  $T_2^*$ . In contrast, by measuring the CPT dip for three pump Rabi frequencies and fitting all traces with the same values of the fitting parameters, we

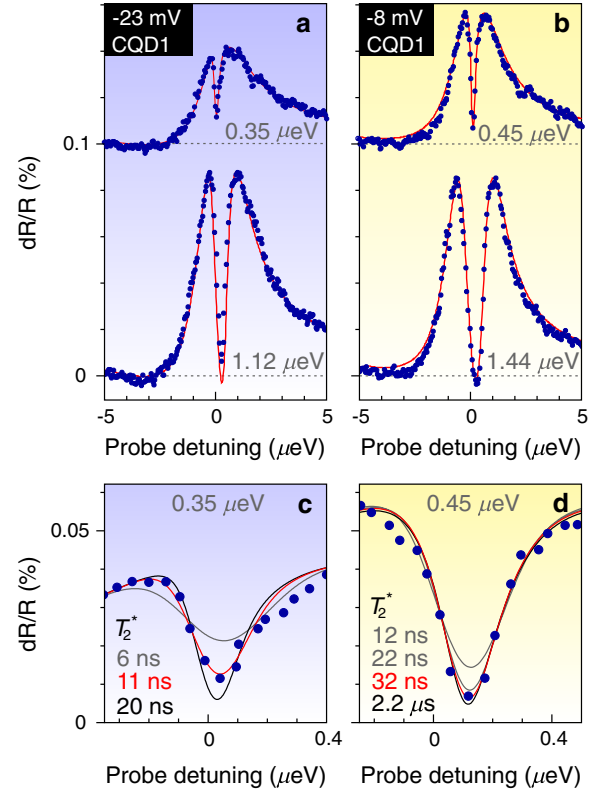


FIG. 3 (color online). Quantitative analysis of the  $T_2^*$  decoherence time in CQD1 at 0.2 T. (a) dR spectra (blue dots) far away from the sweet spot ( $\Delta V = -23$  mV) for two different pump Rabi frequencies  $\Omega_{T_0}$  (indicated in gray). Numerical fits [23] to the data are shown in red. Traces are offset vertically for clarity. (b) dR spectra and fits closer to the sweet spot ( $\Delta V = -8$  mV). (c) Close-up of the upper trace in (a). The spectrum is fitted with different values of  $\Delta V$  while keeping  $T_2^{\text{tunnel}} = 250$  ns constant. From dark gray to red to black:  $\Delta V = -43, -23, -13$  mV, corresponding to the  $T_2^*$  values indicated in the figure. (d) Close-up of the upper trace in (b), fitted with  $\Delta V = -22, -12, -8, 0$  mV.

can extract a single value of  $T_2^*$  for each gate voltage, and at the same time determine that the Gaussian charge fluctuations are the dominant source of decoherence in our case. From this quantitative understanding of the relevant decoherence processes we can extrapolate that in the absence of (co)tunneling,  $T_2^*$  at the sweet spot should well exceed  $1$   $\mu\text{s}$ , limited by second-order charge fluctuations. However, second-order hyperfine processes (not included in the simulations) would in this case limit the achievable coherence time to  $T_2^* \sim 1$   $\mu\text{s}$ .

To demonstrate such long  $T_2^*$  times, we find another coupled QD pair where the sweet spot is further away from the edge of the (1,1) plateau, so that tunneling-induced spin dephasing is strongly suppressed. For this second QD molecule (CQD2), our fitting procedure yields a lower bound on  $T_2^*$  associated with a confidence level calculated from the finite noise in our measurements



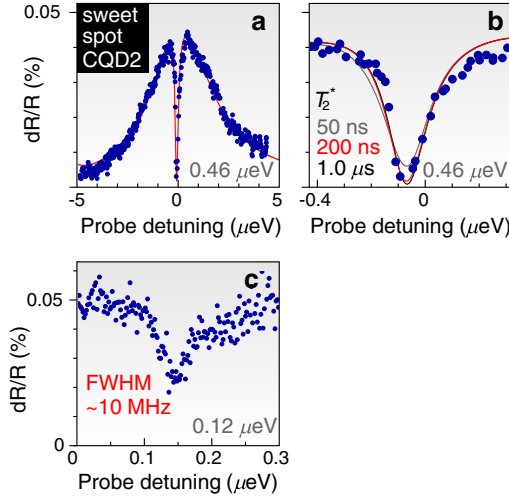


FIG. 4 (color online). Suppressed decoherence close to the sweet spot in CQD2. (a) dR spectra (blue dots) with  $\Omega_{T_0} = 0.46 \mu\text{eV}$  at  $B = 0.2 \text{ T}$ . Because of sample drifts, tuning the gate voltage exactly to the sweet spot is challenging, so we estimate that  $\Delta V = 0 \pm 2 \text{ mV}$ . (b) Close-up of (a). The numerical fits [23] correspond to the  $T_2^*$  values indicated in the figure, with  $T_2^* = 200 \text{ ns}$  fitting best. (c) CPT spectrum for very low pump and probe power ( $\Omega_S \approx \Omega_{T_0} = 0.12 \mu\text{eV}$ ). In this regime, the CPT dip has a full width at half maximum of only  $\sim 10 \text{ MHz}$ .

[Figs. 4(a) and 4(b)]. With a confidence level exceeding 50%, we find that  $T_2^* \geq 200 \text{ ns}$ . This bound on  $T_2^*$  is more than two orders of magnitude longer than previously reported values for coupled electron [14] or hole [16] spins away from the sweet spot; in addition, it is more than an order of magnitude longer than  $T_2^*$  for a single electron [1,2,7,9], and comparable to that of a single hole [5]. Our system thus maintains coherence on time scales that previously required spin echo techniques; the corresponding reduction in overhead can be very beneficial for applications in quantum information processing. Conversely, the long  $T_2^*$  should improve the effectiveness of a spin echo pulse, and could thus lead to even longer spin echo  $T_2$  times. Finally, the potential of our system for high-resolution spectroscopy is highlighted in Fig. 4(c); reducing the pump and probe Rabi frequencies to  $\Omega_S \approx \Omega_{T_0} = 0.12 \mu\text{eV}$  yields a narrow CPT dip with a full width at half maximum of just  $\sim 10 \text{ MHz}$ .

Qubits based on singlet-triplet states in CQDs are subject to the same principal limitation on scalability as single-spin qubits: the difficulty in deterministically positioning multiple CQDs to facilitate two-qubit interactions. On the other hand, two-electron CQD molecules offer several unique advantages in addition to their robustness against both electric and magnetic fluctuations. We find that, in general, the electronic  $g$  factors in each of the two coupled dots are  $\sim 10\%$  different, which detunes the  $T_+ - R_{++}$  from the  $T_0 - R_+$  transition, allowing them to be separately addressed at moderate magnetic fields [see

Supplemental Material [23] Figs. S5(a) and (b)]. To implement single-shot spin readout [28], which requires recycling transitions, the  $S$  population could be directly transferred to the  $R_{++}$  state with a strong laser, and subsequently readout using light scattering on the  $T_+ - R_{++}$  transition. In this sense, the rich optical excitation spectrum of QD molecules in the (1,1) regime combines the advantages of both Voigt [29] and Faraday [30] geometries.

Another very interesting possibility is highlighted in Fig. 2(d) where it can be seen that application of an in-plane magnetic field yields two dark resonances [18]: It has been shown theoretically [31] that by adiabatically changing the laser intensity and phase in a three-laser geometry, it is possible to realize a Hadamard-Berry-phase gate, rotating the system wave function from one dark state to a coherent superposition of the two dark states.

This work is supported by the Swiss National Science Foundation NCCR-QSIT and an ERC Advanced Investigator grant (QON). K. M. W and J. M. E. contributed equally to this work.

---

\*Present address: London Centre for Nanotechnology and Department of Electronic and Electrical Engineering, University College London, London WC1H 0AH, United Kingdom.

- [1] R. Hanson, L. P. Kouwenhoven, J. R. Petta, S. Tarucha, and L. M. K. Vandersypen, *Rev. Mod. Phys.* **79**, 1217 (2007).
- [2] M. H. Mikkelsen, J. Berezovsky, N. G. Stoltz, L. A. Coldren, and D. D. Awschalom, *Nature Phys.* **3**, 770 (2007).
- [3] D. Press, T. D. Ladd, B. Zhang, and Y. Yamamoto, *Nature (London)* **456**, 218 (2008).
- [4] X. Xu, B. Sun, P. R. Berman, D. G. Steel, A. S. Bracker, D. Gammon, and L. J. Sham, *Nature Phys.* **4**, 692 (2008).
- [5] D. Brunner, B. D. Gerardot, P. A. Dalgarno, G. Wüst, K. Karrai, N. G. Stoltz, P. M. Petroff, and R. J. Warburton, *Science* **325**, 70 (2009).
- [6] K. De Greve *et al.*, *Nature Phys.* **7**, 872 (2011).
- [7] J. R. Petta, A. C. Johnson, J. M. Taylor, E. A. Laird, A. Yacoby, M. D. Lukin, C. M. Marcus, M. P. Hanson, and A. C. Gossard, *Science* **309**, 2180 (2005).
- [8] H. Bluhm, S. Foletti, I. Neder, M. Rudner, D. Mahalu, V. Umansky, and A. Yacoby, *Nature Phys.* **7**, 109 (2010).
- [9] D. Press, K. De Greve, P. L. McMahon, T. D. Ladd, B. Friess, C. Schneider, M. Kamp, S. Höfling, A. Forchel, and Y. Yamamoto, *Nature Photon.* **4**, 367 (2010).
- [10] C. Latta *et al.*, *Nature Phys.* **5**, 758 (2009).
- [11] X. Xu, W. Yao, B. Sun, D. G. Steel, A. S. Bracker, D. Gammon, and L. J. Sham, *Nature (London)* **459**, 1105 (2009).
- [12] H. Bluhm, S. Foletti, D. Mahalu, V. Umansky, and A. Yacoby, *Phys. Rev. Lett.* **105**, 216803 (2010).
- [13] D. A. Lidar, I. L. Chuang, and K. B. Whaley, *Phys. Rev. Lett.* **81**, 2594 (1998).
- [14] D. Kim, S. C. Carter, A. Grelich, A. S. Bracker, and D. Gammon, *Nature Phys.* **7**, 223 (2010).

- [15] J. M. Elzerman, K. M. Weiss, J. Miguel-Sanchez, and A. Imamoglu, *Phys. Rev. Lett.* **107**, 017401 (2011).
- [16] A. Greilich, S. G. Carter, D. Kim, A. S. Bracker, and D. Gammon, *Nature Photon.* **5**, 702 (2011).
- [17] E. A. Stinaff, M. Scheibner, A. S. Bracker, I. V. Ponomarev, V. L. Korenev, M. E. Ware, M. F. Doty, T. L. Reinecke, and D. Gammon, *Science* **311**, 636 (2006).
- [18] H. E. Türeci, J. M. Taylor, and A. Imamoglu, *Phys. Rev. B* **75**, 235313 (2007).
- [19] D. Vion, A. Aassime, A. Cottet, P. Joyez, H. Pothier, C. Urbina, D. Esteve, and M. H. Devoret, *Science* **296**, 886 (2002).
- [20] J. Koch, T. M. Yu, J. Gambetta, A. A. Houck, D. I. Schuster, J. Majer, A. Blais, M. H. Devoret, S. M. Girvin, and R. J. Schoelkopf, *Phys. Rev. A* **76**, 042319 (2007).
- [21] J. Vanier, *Appl. Phys. B* **81**, 421 (2005).
- [22] H. J. Krenner, M. Sabathil, E. C. Clark, A. Kress, D. Schuh, M. Bichler, G. Abstreiter, and J. J. Finley, *Phys. Rev. Lett.* **94**, 057402 (2005).
- [23] See Supplemental Material at <http://link.aps.org/supplemental/10.1103/PhysRevLett.109.107401> for details of the materials, methods, and theoretical analysis.
- [24] B. Alén, F. Bickel, K. Karrai, R. J. Warburton, and P. M. Petroff, *Appl. Phys. Lett.* **83**, 2235 (2003).
- [25] M. Fleischhauer, A. Imamoglu, and J. P. Marangos, *Rev. Mod. Phys.* **77**, 633 (2005).
- [26] K.-J. Boller, A. Imamoglu, and S. E. Harris, *Phys. Rev. Lett.* **66**, 2593 (1991).
- [27] J. Houel *et al.*, *Phys. Rev. Lett.* **108**, 107401 (2012).
- [28] A. N. Vamivakas, C.-Y. Lu, C. Matthiesen, Y. Zhao, S. Fält, A. Badolato, and M. Atatüre, *Nature (London)* **467**, 297 (2010).
- [29] X. Xu, Y. Wu, B. Sun, Q. Huang, J. Cheng, D. G. Steel, A. S. Bracker, D. Gammon, C. Emary, and L. J. Sham, *Phys. Rev. Lett.* **99**, 097401 (2007).
- [30] S. T. Yilmaz, P. Fallahi, and A. Imamoglu, *Phys. Rev. Lett.* **105**, 033601 (2010).
- [31] D. Møller, L. B. Madsen, and K. Mølmer, *Phys. Rev. A* **75**, 062302 (2007).